Lithos 216–217 (2015) 338–351

Contents lists available at ScienceDirect

Lithos

journal homepage: www.elsevier.com/locate/lithos

Invited review article

Grain-scale pressure variations in metamorphic rocks: implications for the interpretation of petrographic observations

Lucie Tajčmanová [a,*], Johannes Vrijmoed [a], Evangelos Moulas [a,b]

[a] Department of Earth Sciences, ETH Zurich, Switzerland
[b] Institute of Earth Sciences, University of Lausanne, Switzerland

ARTICLE INFO

Article history:
Received 20 August 2014
Accepted 10 January 2015
Available online 19 January 2015

Keywords:
Equilibrium thermodynamics
Lithostatic pressure
Mechanical equilibrium
Nonhydrostatic thermodynamics
Pressure variations

ABSTRACT

Recent work on mineral reactions and microstructures in metamorphic rocks has focused on forward modelling of phase equilibria and on their description through chemical potential relationships which control mass transfer in rocks. The available thermodynamic databases and computer programs for phase equilibria modelling have significantly improved the quantification and understanding of geodynamic processes. Therefore, our current methodological framework seems to be satisfactory. However, the quantification approaches in petrology focus on chemical processes with oversimplified mechanics. A review of the recent literature shows that mechanical effects in rocks may result in the development of pressure variations even on a hand specimen or grain scale. Such variations are critical for interpreting microstructural and mineral composition observations in rocks. Mechanical effects may influence element transport and mineral assemblage in rocks. Considering the interplay of mechanical properties and metamorphic reactions is therefore crucial for a correct interpretation of microstructural observations in metamorphic rocks as well as for quantification of processes. In this contribution, arguments against pressure variations are inspected and disproved. The published quantification procedure for systems with grain-scale pressure variations is reviewed. We demonstrate the equivalence of using Gibbs and Helmholtz energy in an isobaric system and go on to suggest that Gibbs free energy is more convenient for systems with pressure variations. Furthermore, we outline the implications of the new quantification approach for phase equilibria modelling as well as diffusion modelling. The appropriate modification of a macroscopic flux for a system with a pressure variation is derived and a consequence of using mass or molar units in diffusional fluxes is discussed. The impact of ignoring grain-scale pressure variations on geodynamic modelling and our understanding of the processes in the Earth's interior is assessed. We show that if a pressure variation is overlooked, the error in depth estimates from crustal metamorphic rocks could be as large as the thickness of the crust.

Contents

* Corresponding author.
E-mail address: lucataj@gmail.com (L. Tajčmanová).

http://dx.doi.org/10.1016/j.lithos.2015.01.006

1. Introduction

Many phenomena in the Earth's interior can be explained by mineral reactions and phase transformations. Mineral reactions greatly affect the physical properties of Earth materials and impose first order controls on geodynamic processes. Differences in mechanical properties due to reaction, such as relative differences in viscosity between magma and the rock from which it melts, may reach over ten orders of magnitude (e.g. Cruden, 1990; Dimanov et al., 2000; Rosenberg and Handy, 2005). High mechanical strength may suppress reaction associated with large volumetric changes, thus preserving rock history and properties (Liu et al., 1998; Morris, 2002, 2014; Mosenfelder et al., 2000; Schmid et al., 2009; Zhang, 1998). Recent observations show that mechanically maintained pressure variations can be significant even on a micro-scale. Current analytical and imaging techniques allow direct investigation of minerals under residual pressure (Fig. 1a,b; Howell, 2012; Howell et al., 2010; Nasdala et al., 2005). High residual pressures (GPa level) are still present in rocks at ambient conditions, for example the ultrahigh pressure mineral, coesite, is preserved as inclusions in garnet at the Earth's surface (Parkinson, 2000), as well as residual pressure in quartz inclusions in garnet (e.g. Enami et al., 2007; see also Moulas et al., 2013, and references therein). Furthermore, few studies document that ultrahigh-pressure (UHP) phases can be preserved even within a polycrystalline matrix (Fig. 1c; Ji and Wang, 2011; Liou and Zhang, 1996; Yang et al., 2014). Experimental studies also suggest a development of grain-scale heterogeneous pressure as revealed, for example, by the coexistence of low and high pressure SiO_2 polymorphs in quartzite deformation experiments (Hirth and Tullis, 1994). Given that the magnitude of metamorphic pressure provides the key constraint (via depth of burial) for geodynamic reconstructions of orogens, ignoring such pressure variations in petrological analysis is likely to significantly influence the quality and general results of these reconstructions.

Metamorphic petrologists as well as structural geologists bring important observational constraints for geodynamic models. If properly quantified and interpreted, fabrics and microstructures in rocks provide fundamental constraints on lithospheric evolution. However, in the context of complex rock fabrics and microstructures, application of inappropriate quantification approaches may lead to flawed interpretations. The classical view of metamorphic microstructures assumes fast relaxation of stresses (therefore constant pressure) as well as constant temperature. In this case, chemical diffusion is the only limiting factor in the thermodynamic equilibration of the microstructure (Ashworth and Birdi, 1990; Fisher, 1973; Joesten, 1977). The presence of zoned porphyroblasts, coronal structures and spatially organized reaction zones thus points to the preservation of an apparent disequilibrium in the microstructures (e.g. Carlson, 2002 and references therein). This classical view is limited because it precludes the possibility that metamorphic microstructures involve mechanically maintained pressure variations. Several quantitative studies have considered mechanical effects on mineral reactions (Ferguson and Harvey, 1980; Fletcher, 1982; Fletcher and Merino, 2001; Milke et al., 2009; Rutter, 1976; Schmid et al., 2009; Wheeler, 1987). None of these studies focused on a mechanical consequence for diffusion and the resulting chemical redistribution between and in minerals. Recently, Tajčmanová et al. (2014) focused on a complementary scenario to the classical diffusion controlled view, where fast diffusion is accompanied by slow stress relaxation. They point out that chemical zoning in grains (e.g. of plagioclase) surrounding a high-pressure phase (e.g. kyanite), associated with decompression at high temperature (>700 °C), may reflect pressure variations on that scale. Such a microstructure then need not be interpreted as a preserved chemical disequilibrium (i.e. by sluggish chemical diffusion) but can be fully quantified via appropriately modified equilibrium thermodynamics. The importance of mechanical effects on metamorphic reactions has also been suggested recently in the context of nonhydrostatic thermodynamics (Wheeler, 2014). Wheeler (2014) endeavours to show that the effect of differential stress on the inferred pressure conditions, under which a metamorphic reaction takes place, can be as dramatic as several GPa. However, this theory contradicts the available experimental data and its feasibility is discussed below.

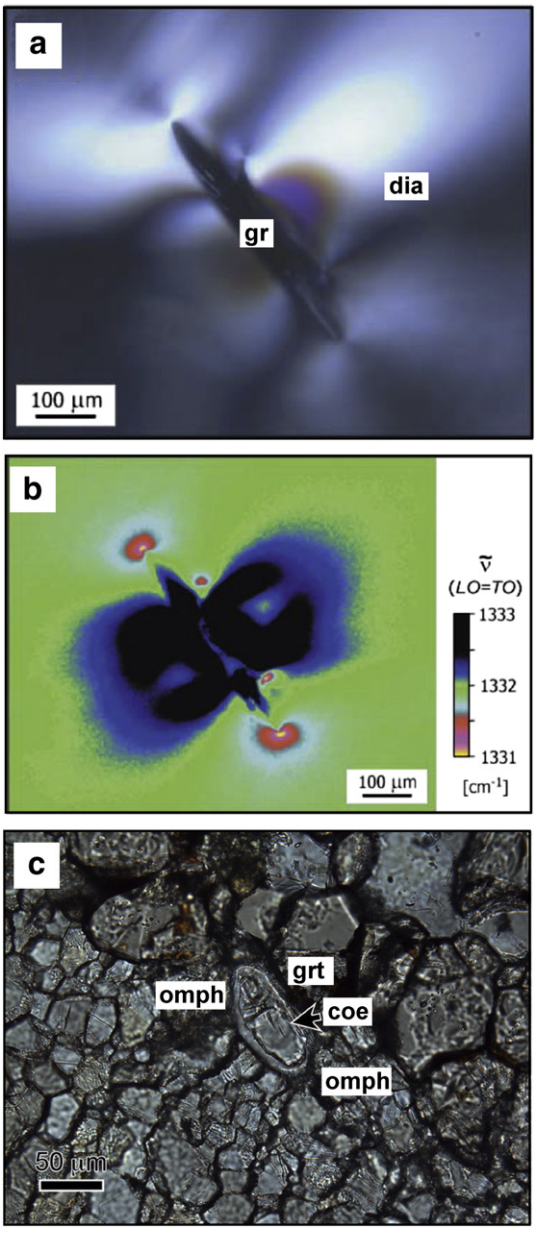

Fig. 1. a) Crossed-polarized light photomicrograph of graphite inclusion in diamond and b) Raman map of the same area portraying the distribution of remnant internal pressure - the blue-black region based on the frequency of the *LO-TO* photon (modified from and see Nasdala et al., 2005 for details). c) Intergranular coesite with thin rim of quartz (modified from Yang et al., 2014). Abbreviations: gr = graphite; dia = diamond; omph = omphacite; grt = garnet; coe = coesite.

Whereas observational and theoretical results obtained so far have provided insights into the interplay between deformation and mineral reaction, recent developments in conceptual models have opened new horizons in understanding mineral reaction mechanisms in the Earth's lithosphere. It is timely that these latest breakthroughs in considering metamorphic microstructures, in particular involving grain-scale pressure variations, are reviewed here.

2. The role of pressure: from petrology to geodynamic reconstructions

2.1. Pressure and stress in space and time

Stress has dimensions of force per unit area. At every point of a body, a unit area can be specified in terms of the direction of its normal vector. Stresses acting on differently oriented unit areas at the same point of a solid need not be equal. On the other hand, pressure being an average over directions of normal stresses acting at a point of a solid body is direction independent (Fig. 2a). A solid body can be under hydrostatic conditions if all stresses applied on it are equal in magnitude and normal to its surface (Fig. 2a). If stresses acting on the body are different in different directions, then the material is under nonhydrostatic stress (Fig. 2b). In the absence of shear stresses (i.e., when coordinate axes are parallel to the principal stress axes), the difference between the maximum and minimum values of normal stress, i.e. σ_{xx} and σ_{yy}, is the differential stress (σ_d). Differential stress controls deformation (change of shape), whereas mean stress is associated with volume change.

In the simplified scenario portrayed in Fig. 2a, it is assumed that the state of stress is homogeneous and density is constant within the body. Static fluids have zero differential stress. Such fluids are in static equilibrium (subjected to gravity only) and their pressure can be calculated from the hydrostatic formula ($P = \rho gh$). Similarly, if rocks are assumed to have a negligible differential stress, pressure is lithostatic (influenced by gravity only) and the hydrostatic formula can be applied to them as well. The maximum differential stress that rocks can sustain is related to their strength. One of the important factors that can significantly influence the rock strength is the presence of porous fluids that can result in hydro-fracturing. Hydro-fracturing in metamorphic rocks led to the interpretation that the whole lithosphere is not able to support differential stresses larger than 20 MPa (Etheridge, 1983). Such a view of rocks is convenient because the pressure obtained from geobarometric estimates can then be directly converted to depth via the lithostatic formula ($P = \rho gh$) and thus have a direct application in geodynamic models.

However, the question arises whether the lithostatic assumption is always applicable. In fact, the spatial distribution of pressure in the lithosphere is not only likely to be heterogeneous but also changes with time. Metamorphic rocks evolve in static conditions and also during deformation as reflected by their microstructures. Grain-scale heterogeneous pressure patterns have been documented in petrology studies, *in situ*, as noted above (Fig. 1). Therefore, the actual pressure (the mean normal stress) may deviate from the lithostatic pressure by a positive (overpressure) or a negative (underpressure) magnitude (e.g. Mancktelow, 2008).

2.2. A paradigm shift regarding lithostatic pressure

Tectonic overpressure has been mostly suggested for the formation of high to ultrahigh-pressure (UHP) rocks (e.g. Chopin, 1984; Rutland, 1965; Smith, 1984). The main motivation for this was the lack of structures and rock mass which would explain the depths implied by thermodynamic pressure given by geobarometry (Bailey et al., 1964; Brace et al., 1970). However, qualitative arguments to discount overpressure have been enumerated at various times (Brace et al., 1970; Green, 2005; Schreyer, 1995). The most common reasoning against tectonic overpressure is that rocks are weak (i.e. can sustain only low differential stress) and thus cannot sustain large pressure variations. Because such a statement seems to be critical for our correct understanding of Earth processes, we examine its legitimacy below.

The coesite-bearing quartzite from Dora Maira in the Alps opened a discussion whether the presence of UHP minerals may be a result of a micro-scale intracrystalline tectonic overpressure or rather a result of a homogeneous lithostatic pressure during deep subduction (e.g. Chopin, 1984; Smith, 1984). Schreyer (1995) claimed that a rock that contains weak minerals such as micas or talc cannot hold overpressure during its prograde evolution because it is weak. The phases (coesite and diamond) were thus interpreted to be actually formed at UHP depths (e.g. >70–80 km), as given by the lithostatic formula ($P = \rho gh$), and preserved only when entrapped in strong host minerals such as garnet, during decompression from those conditions. Similarly, Brace et al. (1970) argued that the degree of overpressure depends on the rock's strain rate and temperature. Even though their experiments on metagreywacke showed differential stresses up to 1 GPa, they suggested that rocks in nature have practically no strength due to reactions taking place in them. In fact, this suggestion was not supported by their experimental results. Interestingly, recent work on the rheology of omphacite aggregates shows that these minerals can sustain GPa-level stresses as shown by micromechanical-based extrapolations to geological conditions (Moghadam et al., 2010), not inconsistent with the Brace et al. (1970) experimental data. Another indication of significant rock strength may be obtained by stress drop estimates from deep earthquakes. Natural observations of faulting associated with pseudotachylite formation were used by Andersen et al. (2008) to infer stress drop during intermediate to deep earthquakes in an Alpine subduction setting. Their minimum estimates suggest that upper mantle rocks can sustain differential stress of at least 0.22–0.58 GPa.

Green (2005) was another proponent of the lithostatic pressure view. However, the arguments based on nonhydrostatic thermodynamics (e.g. Kamb, 1961) referred to in his work are contradictory. He attempts to invalidate overpressure by a qualitative contemplation of different mineral interfaces being connected with a different stress distribution. Such a heterogeneous stress distribution then influences the crystallization of phases based on which stability field the normal stress places them. This actually supports the idea of grain-scale pressure variations rather than being an argument for the lithostatic view. Similar variations have been claimed recently by Wheeler (2014) where it is suggested that the large impact of nonhydrostatic stress on phase equilibria clearly rules out the pressure to depth conversion approach defended by Green (2005). Alternatively, Ji and Wang (2011) used the concept of interfacial friction-induced pressure to explain the large

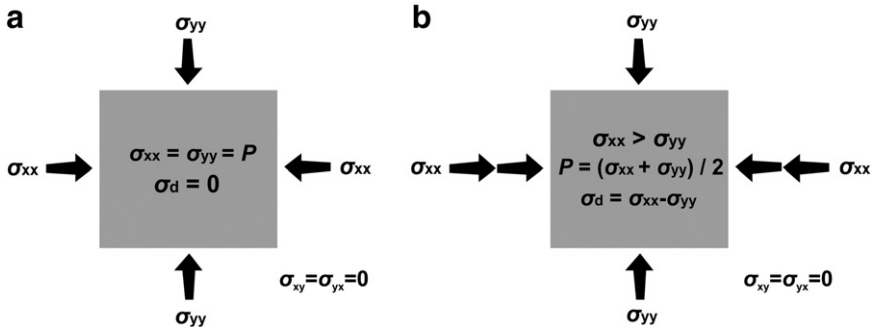

Fig. 2. Simplified sketch of a 2D body under a) hydrostatic stress (meaning homogeneous stress state), b) nonhydrostatic stress. Pressure is defined as mean stress. The subscripts x and y refer to the coordinate frame. σ_{xy} and σ_{yx} are stresses applied parallel to the surfaces, i.e. shear stresses.

pressure deviations from the lithostatic value along grain boundaries for intergranular coesite.

On a geodynamic scale, the lithostatic view is inconsistent with the horizontal force balance needed to support mountains and their roots (Molnar and Lyon-Caen, 1988; Schmalholz et al., 2014a, see also Turcotte and Schubert, 2002, page 136). Petrini and Podladchikov (2000) showed that in homogeneous crust, overpressure can be as large as the lithostatic load if strong lithologies are involved (i.e. rocks that can sustain large differential stress). Furthermore, Petrini and Podladchikov (2000) model for lower crustal rocks with zero differential stress (simulating an infinitely weak rock) also shows a noteworthy deviation from lithostatic conditions. These results are also supported by studies that quantify the overpressure in subduction channels (Burg and Gerya, 2005; Gerya et al., 2008; Li et al., 2010; Mancktelow, 1995). Recently, lithospheric-scale dynamic modelling has been performed that further questions the "weak rock" idea (Schmalholz and Podladchikov, 2013). Their modelling implies large-scale pressure heterogeneities during lithospheric shortening. During the formation and weakening of crustal-scale shear zones, the pressure (mean stress) in the shear zones increased, while the differential stress decreased, so as to maintain a horizontal force balance. More specifically, if differential stress becomes negligible, a rock has to change its pressure to maintain the total force balance (see Fig. 3 and explanation in section below). This invalidates all of the qualitative statements above (e.g. Brace et al., 1970; Green, 2005; Schreyer, 1995). Moreover, Schmalholz et al. (2014b) could obtain overpressure corresponding to the coesite stability field even at middle crustal depths. The pressure variation predicted by the model of Schmalholz et al. (2014b) is likely to be on outcrop-scale or larger. However, the same force balance logic may be applied on a grain-scale, as shown in the next section.

2.3. Pressure variations on a grain-scale

The stress and pressure distribution at the contact of two strong minerals separated by a weak phase can be considered in terms of a horizontal force balance. Following Fig. 2b, the total stress applied to the sides of the elementary volume has to remain constant across this volume (Fig. 3a). The total horizontal stress is decomposed into pressure (P) and the remaining part is the so-called deviatoric stress (τ_{xx}).

$$\sigma_{xx} = P + \tau_{xx} \quad (1)$$

The sign convention that stress is positive in compression is followed (Turcotte and Schubert, 2002, p.136). If a weak zone is introduced in the elementary volume (Fig. 3b), the deviatoric part of the total horizontal stress drops. Therefore, to maintain the total horizontal stress constant, pressure must increase in the weak zone. This is also valid for the large scale tectonic overpressure, as shown by Schmalholz and Podladchikov (2013).

If the setting from Fig. 3 is expanded into the thin section scale where different mineral grains have different mechanical properties (Fig. 4) the resulting stress and pressure can vary locally even within a single grain. To illustrate this we consider a rock which is made of three different minerals characterized by different viscosities (Fig. 4a). The phases are considered to be vertically shortened leading to the development of heterogeneous stress and pressure patterns (Fig. 4b, c). The result shows that small differential stress in some minerals does not mean that rocks cannot sustain large over/underpressure. Furthermore, due to very high viscosities of most of the main rock-forming minerals, the viscous relaxation is assumed to be very slow (Dabrowski et al., in press; Zhang, 1998). Therefore, under the assumption of infinitely slow viscous relaxation, the main reason for maintaining the pressure variation is that the pressure/stress state of the minerals is controlled by the force balance. As metamorphic rocks are subjected to deformation (and thus differential stress) on geological timescales, pressure variations can also be maintained on geological timescales (Moulas et al., 2014).

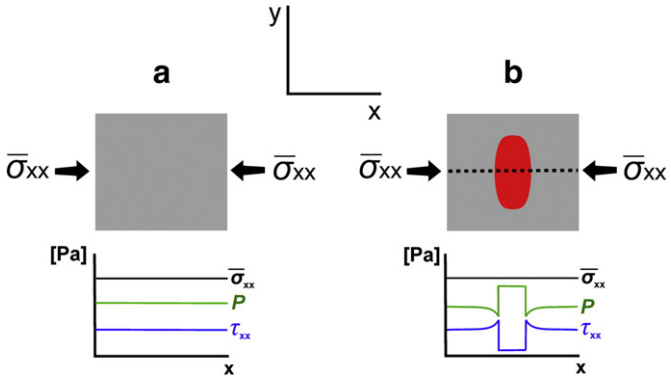

Fig. 3. Schematic diagram showing pressure variations developed in a weak zone of a body in the absence of shear stresses at the boundaries. a) In a small homogeneous elementary volume the horizontal total stress ($\overline{\sigma}_{xx}$, integrated over y) has to remain constant in order to keep the horizontal force balanced. b) A weak zone (small deviatoric stress τ_{xx}) is considered to lie within the elementary volume considered in a). The weak zone is characterized by the red ellipse. Then, pressure has to increase within the weak zone in order to satisfy the horizontal force balance. The sign convention followed here is after Turcotte and Schubert (2002, p.136; stress is positive in compression). The dashed line represents a line along which τ_{xx} and P have been calculated. For the calculation of pressure and stress fields around an elliptical weak zone see Schmid and Podladchikov (2003) and Moulas et al. (2014).

3. Quantification for systems with pressure variations

In the previous section, it has been suggested that pressure variations can be mechanically maintained on geological timescales and on various length scales even in weak rocks. The mechanical models are also supported by direct observations of pressure variations in natural and experimental samples. The important question is how large the pressure variations can be and how much they can influence the petrology interpretations that are then used in geodynamic reconstructions. In other words, how flawed is the conventional constant pressure approach. To tackle this, an appropriate thermodynamic formulation for quantification of microstructures reflecting pressure variations must be applied and tested. Such a formulation should represent a bridge between the likely chemical and mechanical processes involved, and thus should allow an appropriate use of petrographic observations for quantifying processes.

Many attempts have been made in this direction using either equilibrium thermodynamics for thermo-barometric purposes or non-equilibrium thermodynamics to explain steady (stationary) state systems (e.g. Fisher, 1973; Nishiyama, 1983). Furthermore, closely related to the previous section on the effects of stress, the thermodynamic approaches may differ based on whether hydrostatic or nonhydrostatic conditions are assumed. Therefore, the most common thermodynamic approaches in petrology are reviewed in the context of their applications for the systems under pressure variations.

3.1. Hydrostatic versus nonhydrostatic approaches

Classical thermodynamic calculations in petrology assume hydrostatic stress conditions. Hydrostatic thermodynamics creates a basis for the most common phase equilibria quantification methods in petrology mentioned earlier (e.g. Connolly, 2009; de Capitani and Petrakakis, 2010; Powell et al., 1998). In fact, all the mineral end member properties, such as volume, in thermodynamic databases are derived from experiments performed under hydrostatic

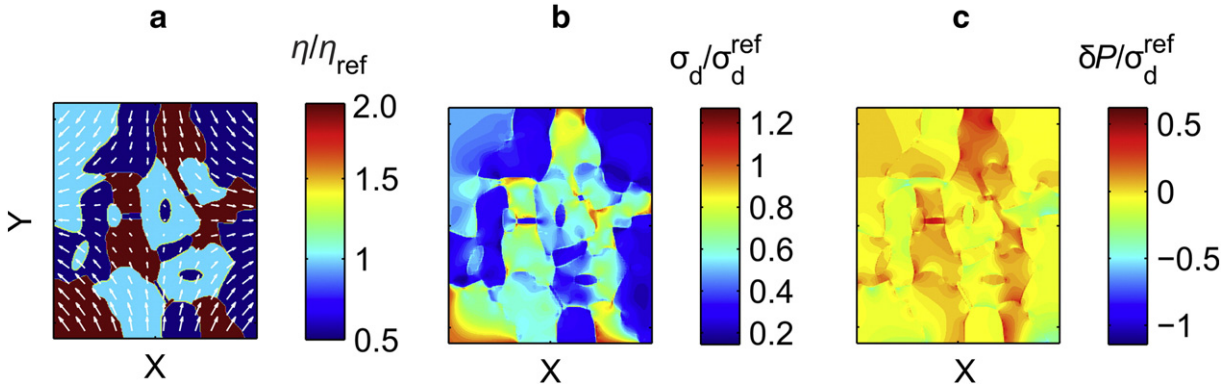

Fig. 4. Computed model of a polycrystalline rock under vertical shortening. The model was computed using the code of Räss (2013). The spatial coordinates are normalized to the size of the model (i.e. dimensionless). The rheology is assumed to be linear viscous. a) Viscosity (η) variation among mineral grains. All viscosities are normalized to a reference viscosity (η_{ref}). White arrows indicate local velocity vector. b) Differential stress (σ_d) computed for different parts of the microstructure. Grains with high viscosity can support higher differential stress. The differential stress supported by the strong grain in the left, lowermost part of the figure was used as a reference (σ_d^{ref}). c) Pressure deviation (δP) computed for different parts of the microstructure. The regions of small differential stress can also develop large pressure deviations. The pressure deviation is the difference from the pressure of the grain shown in the left, lowermost part of the figure and it is normalized over the differential stress of that grain (σ_d^{ref}).

conditions (under low differential stress). Experimental diagrams can be then compared consistently only against calculations based on hydrostatic thermodynamics. However, hydrostatic thermodynamics was derived for fluids and gases (Gibbs, 1906). The question how a thermodynamic equilibrium between nonhydrostatically stressed solids should be formulated has concerned researchers ever since Gibbs (for details see the review of Paterson (1973)). Gibbs (1906) in his chapter "On the equilibrium of heterogeneous substances" discussed the problem of equilibrium between a nonhydrostatically stressed solid and its solution in hydrostatic fluid. However, he attached a chemical potential only to the dissolved substance in hydrostatic fluid and not to the nonhydrostatically stressed solid itself. As the explicit treatment of nonhydrostatic solid-solid scenario is missing in the work of Gibbs, many researchers have attempted to formulate the nonhydrostatic chemical potential. However, the attempts have been criticised as early as Verhoogen (1951) and Kamb (1961).

Pressure variations and nonhydrostatically stressed systems are closely related to each other. A full review of the nonhydrostatic literature is beyond the scope of this work (see Grinfeld, 1991, pp. 125–132 for more details). To illustrate the relevance of nonhydrostatic thermodynamics in the quantification of petrographic observations, the most recent nonhydrostatic contribution by Wheeler (2014) is reviewed here. Wheeler (2014) proposed a new theory on the effects of differential stress on metamorphic reactions. This new theory suggests that a small amount of differential stress can cause an apparent pressure shift of a metamorphic reaction in the order of 10 times the differential stress. For example, 0.1 GPa differential stress can result in approximately 1 GPa apparent pressure shift of the reaction line in a *P-T* space. If this theory had been proved, it would have had a "dramatic" effect on the interpretation of mineral textures that recrystallized under any (even low) differential stress.

In order to verify the theory proposed by Wheeler (2014), a calculation for a differential stress of 0.1 GPa has been performed to illustrate its effect on the quartz-coesite reaction (Fig. 5). The calculation shows the apparent shift of the quartz-coesite reaction from hydrostatic conditions. There are two shifts that can be observed. The first is represented by a precipitation of coesite during forceful crystallization (quartz dissolves at faces perpendicular to σ3 and coesite precipitates at faces perpendicular to σ1). The second is characterized by a pressure solution (quartz dissolves at faces perpendicular to σ1 and coesite precipitates at faces perpendicular to σ3). According to Wheeler, the apparent shift of the quartz to coesite transition is approximately 10 times the differential stress value. This implies that for differential stress of 0.1 GPa, the total uncertainty of the quartz-to-coesite transition corresponds up to 2 GPa (±1 GPa). Our calculation following the theory of Wheeler (2014) is compared with the experimental results of Hirth and Tullis (1994). Here, we follow Feynman's dictum that no matter how elegant a theory is, if it disagrees with experiment, it is flawed (Feynman, 1967).

Hirth and Tullis's experiments involved the uniaxial compression of quartzite samples under high ($\sigma_2 = \sigma_3 \approx 1.3$ GPa) confining pressures. They found that coesite formed under high ($\sigma_d \approx 1.5$ GPa) differential stress at the faces perpendicular to σ_1 only when the maximum principal stress (σ_1) of the experiment was above the quartz-coesite transition determined by hydrostatic experiments. In Fig. 5, solid dots represent the experiments where coesite was observed in the lab in experiments under such large differential stresses (Hirth and Tullis, 1994). Furthermore, Hirth and Tullis (1994) ran several experiments under different stress conditions and they documented no sensitivity of the reaction location to differential stress. The observation of coesite occurs under exactly the same maximum principal stress (σ_1) as predicted by hydrostatic thermodynamics (see experiments at 700 °C) suggesting that in this case the effect of differential stress did not influence the location of the equilibrium. In addition, it is noted that in those experiments the differential stress was more than 1.5 GPa therefore the possible uncertainty in the quartz to coesite reaction as suggested by Wheeler (2014) would be in the order of

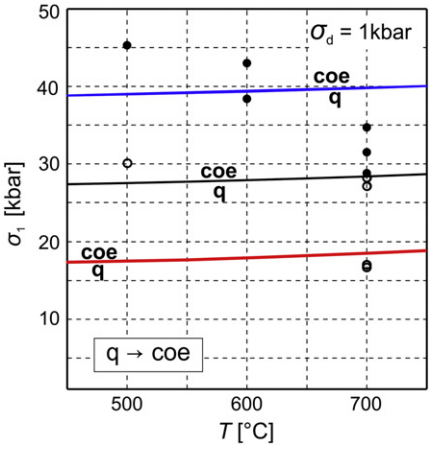

Fig. 5. The effect of differential stress on the quartz (q) to coesite (coe) transition based on Wheeler (2014). The black line is the reference at σ1 = σ2 = σ3 (hydrostatic conditions). The red line represents the lower shift of the reaction due to pressure solution and the blue line represents the shift of the reaction line based on forceful crystallization. The differential stress is assumed to be 1 kbar. The circles represent the experimental results of Hirth and Tullis (1994). Filled circles indicate the presence of coesite preferentially forming at faces perpendicular to σ1. Open circles indicate the presence of quartz. The thermodynamic calculations were done using the thermodynamic database of Holland and Powell (1998), following the approach of Wheeler (2014).

±20 GPa. Such an inconsistency between the theoretical prediction and experimental results suggests that the prediction of the nonhydrostatic approach of Wheeler is highly unlikely.

The comparison above shows that, in the sense of Feynman's dictum, the theory of Wheeler (2014) is flawed. In fact, it confirms the general weak point of many nonhydrostatic-thermodynamics formulations that their validity has not been fully verified so far (Schmalholz and Podladchikov, 2014). Therefore, an appropriate theory and practical application of nonhydrostatic thermodynamics is still open.

3.2. Appropriate thermodynamic functions

In petrology, equilibrium is commonly determined by either Gibbs or Helmholz free energy minimization depending on a particular set of variables (i.e. in terms of *P*, *T or V*, *T* respectively). In the following chapter, a constrained minimization using Lagrange multipliers is documented and both thermodynamic potentials are compared in order to show their equivalence and to evaluate their suitability for systems under a pressure variation.

Gibbs energy (G), as a function of *P* and *T*, can be used for determining the stable mineral assemblage under specified *P-T* conditions. The mineral assemblage that has the minimum Gibbs energy is the stable one (Fig. 6a). The common-tangent approach can be applied to infer compositions of phases at the equilibrium state. The validity of such a construction can be proved by showing its equivalence to Gibbs energy minimization constrained by system composition using Lagrange multipliers. See Table 1 for a complete list of symbols.

The first step is to define the Gibbs energy of the system (G_{sys}), considering a two phase binary system

$$G_{sys} = \alpha_1 g_1 + \alpha_2 g_2 \tag{2}$$

where α_1 and α_2 are the mass proportions of phase 1 and 2 (i.e. two minerals) and g_1 and g_2 are the Gibbs energies of each phase, respectively.

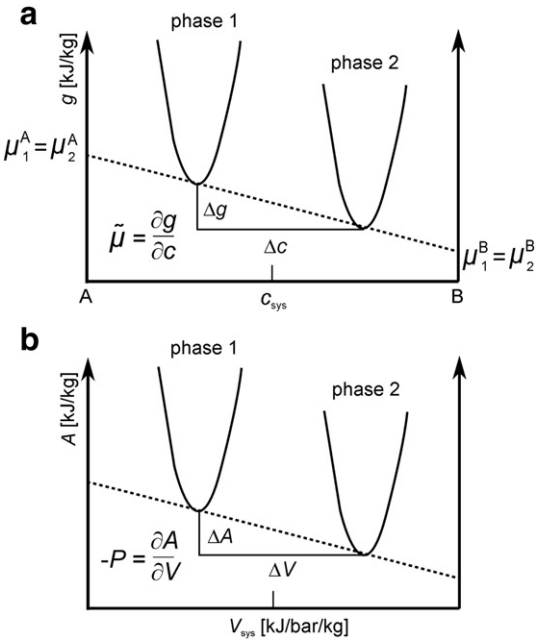

Fig. 6. a) A diagram of Gibbs energy versus composition portraying two binary phases in thermodynamic equilibrium. Pressure and temperature are constant. The composition of the system is represented by C_{sys}. In such as system, the condition for equilibrium is that the chemical potential for the component *A* (μ^A) has to be equal in every phase. Similarly, μ^B has to be equal in every phase as well. b) A diagram of Helmholtz energy versus volume for a system (V_{sys}) involving two phases in thermodynamic equilibrium at constant temperature. The minimum of Helmholtz energy in such a system is represented by the common-tangent which documents that the two phases correspond to the same pressure. Graphical correlation of the two diagrams gives $\tilde{\mu}$ equivalent to $-P$.

Table 1. Symbols and units.

Symbol	Description	Unit
T	Temperature	K
P	Pressure	Pa
R	Universal gas constant	J/mol/K
σ_{xx}	Component of stress tensor	Pa
τ_{xx}	Component of deviatoric part of the stress tensor	Pa
η	Viscosity	Pa s
G_{sys}	Partial Gibbs energy of the system	J/kg
g_i	Partial Gibbs energy of phase *i*	J/kg
α_i	Proportion of phase *i in the system – dimensionless*	[kg/kg]
c_{sys}	Concentration (mass fraction) of a component in the system – *dimensionless*	[kg/kg]
c_i	Concentration (mass fraction) of a component in phase *i – dimensionless*	[kg/kg]
λ_k	Lagrange multiplier for constraint *k*	-
μ_i^A	Chemical potential of component *A* in phase *i*	J/kg
A_i	Partial Helmholtz energy of phase *i*	J/kg
V_i	Partial volume of phase *i*	m^3/kg
P_i	Pressure of phase *i*	Pa
$\bar{c}^A$	Molar concentration (fraction) of component *A*	[moles/moles]
$\bar{\mu}^0(T,P)^A$	Standard molar chemical potential of component *A*	J/mol
$\bar{g}$	Partial molar Gibbs energy	J/mol
a_A	Activity of end member (component) A	-
J_A	Mass flux of component *A*	kg/m^2/s
D	Diffusion coefficient	m^2/s
ρ^A	Density of end member (component) A	kg/m^3
$\bar{V}^A$	Molar volume of end member (component) A	m^3/mol
M^A	Molar mass of end member (component) A	kg/mol

For the minimization, to determine the equilibrium for a specific system composition, the following two constraints must be considered

$$c_{sys} = \alpha_1 c_1 + \alpha_2 c_2 \tag{3}$$

where c_{sys} is the chemical composition of the system and *c* is a chemical composition (as a mass fraction, not the commonly used mole fraction) of the phase with mass proportion α, and

$$1 = \alpha_1 + \alpha_2 \tag{4}$$

Now the function to be minimized is modified by introducing Lagrange multipliers ($\lambda_{1,2}$).

$$L = G_{sys} + \lambda_1(\alpha_1 + \alpha_2 - 1) + \lambda_2\left(\alpha_1 c_1 + \alpha_2 c_2 - c_{sys}\right) \tag{5}$$

Such a function can be minimized by setting the partial derivatives with respect to the unknowns to zero and solving the system of equations. This results in six equations with six unknowns.

$$\frac{\partial L}{\partial \alpha_1} = g_1 + \lambda_1 + \lambda_2 c_1 = 0 \tag{6}$$

$$\frac{\partial L}{\partial \alpha_2} = g_2 + \lambda_1 + \lambda_2 c_2 = 0 \tag{7}$$

$$\frac{\partial L}{\partial c_1} = \lambda_2 \alpha_1 + \alpha_1 \frac{\partial g_1}{\partial c_1} = 0 \tag{8}$$

$$\frac{\partial L}{\partial c_2} = \lambda_2 \alpha_2 + \alpha_2 \frac{\partial g_2}{\partial c_2} = 0 \tag{9}$$

$$\frac{\partial L}{\partial \lambda_1} = \alpha_1 \ + \alpha_2 - 1 = 0 \tag{10}$$

$$\frac{\partial L}{\partial \lambda_2} = \alpha_1 \ c_1 + \alpha_2 \ c_2 - c_{sys} = 0 \tag{11}$$

Solving Eqs. (6) and (9) for λ_1 and λ_2 respectively gives:

$$\lambda_1 = -g_1 + c_1 \frac{\partial g_2}{\partial c_2}$$
$$\lambda_2 = -\frac{\partial g_2}{\partial c_2} \quad (12)$$

Substitution of λ_1 and λ_2 into Eq. (7) leads to

$$g_2 - g_1 + c_1 \frac{\partial g_2}{\partial c_2} - c_2 \frac{\partial g_2}{\partial c_2} = 0 \quad (13)$$

Substitution of λ_2 into Eq. (8) and rearranging gives

$$\frac{\partial g_1}{\partial c_1} = \frac{\partial g_2}{\partial c_2} \quad (14)$$

Therefore, at equilibrium the local slopes of the Gibbs energy of each phase are equal. Using this by substituting Eq. (14) in (13) and rearranging gives:

$$\frac{g_1 - g_2}{c_1 - c_2} = \frac{\partial g_1}{\partial c_1} = \frac{\partial g_2}{\partial c_2} \quad (15)$$

This is the tangent construction involving $\Delta g/\Delta c$ as is familiar in *G-C* diagrams (Fig. 6a).

Assuming that each phase is composed of chemical components *A* and *B* and rearranging Eq. (15) for a component *A* gives equations for chemical potentials (μ) of component *A*

$$\underbrace{g_1 - c_1 \frac{\partial g_1}{\partial c_1}}_{\mu_1^A} = \underbrace{g_2 - c_2 \frac{\partial g_2}{\partial c_2}}_{\mu_2^A} \quad (16)$$

To see the equivalence between chemical potentials of component *B*, it is convenient to add Eq. (14) to (16). This gives (e.g. Hillert, 2007, p. 65)

$$\underbrace{g_1 + (1 - c_1)\frac{\partial g_1}{\partial c_1}}_{\mu_1^B} = \underbrace{g_2 + (1 - c_2)\frac{\partial g_2}{\partial c_2}}_{\mu_2^B} \quad (17)$$

The above derivation shows that the constrained Gibbs energy minimization yields $\Delta\mu$ for each component equal to zero. Interestingly, for a unary system, the derivative part disappears, leading to

$$g_1 = g_2 \quad (18)$$

The Gibbs energy is particularly useful for systems with constant pressure (and temperature). In the nonhydrostatic literature and for isochoric systems, the Helmholtz energy (A) as a function of specific volume or density and temperature is considered to be more appropriate for a description of coexisting phases in equilibrium. For a specific system volume lying between the volumes of the two phases being considered, equilibrium is attained when a minimum of the Helmholtz energy is reached (Fig. 6b). If Helmholtz energy is considered, the pressure of the coexisting phases is represented by a commontangent (Fig. 6b). In fact, under a constrained system volume, the minimum of the Helmholtz energy (for a unary system) is analogous to the minimum of the Gibbs energy constrained by the system composition. The minimum of Helmholtz energy (A) can also be calculated via Lagrange multipliers when, in the above shown derivation, Gibbs energy is substituted by Helmholtz and composition by partial volume (e.g. Eq. (15)). Such a derivation leads to the same result as that with Gibbs energy and documents the equivalence of the two functions:

$$\frac{A_1 - A_2}{V_1 - V_2} = \frac{\partial A_1}{\partial V_1} = \frac{\partial A_2}{\partial V_2} \quad (19)$$

Using the thermodynamic relationship from Fig. 6b, the derivatives can be rewritten as

$$-P_1 = \frac{\partial A_1}{\partial V_1} = \frac{\partial A_2}{\partial V_2} = -P_2 \quad (20)$$

Eqs. (19) and (20) are used to give a change of Helmholtz free energy at constant temperature (e.g. Cemič, 2005; p. 167)

$$\Delta A = -P\Delta V \quad (21)$$

Considering Eq. (21) and rearranging using Eq. (20) gives

$$A_1 + PV_1 = A_2 + PV_2 \quad (22)$$

Expression 22 gives $g_1 = g_2$ which is equivalent to Eq. (18). Therefore, the condition for chemical equilibrium is equivalent in both isobaric and isochoric unary systems.

In fact, minimization of Helmholtz energy predicts that the two phases in thermodynamic equilibrium in an isochoric system have the same pressure (Fig. 6b). Therefore, Helmholtz energy cannot be directly applied to the description of equilibrium under pressure variations without either an appropriate modification (Gibbs, 1906) or an appropriate constraint (Vrijmoed and Podladchikov, 2014). Gibbs (1906) realized that the chemical potential can be influenced by external forces such as gravity and thus he modified the equation for the chemical potential by adding a gravity term. Such a modification has been then applied to Gibbs energy (Lewis and Randall, 1923) as well as to Helmholtz energy for centrifugation equilibrium problems (Castier and Tavares, 2005; Espósito et al., 2000). However, the application has focused mostly on fluids, proteins and gases with the assumption of continuous pressure at equilibrium (Gibbs, 1906). In solid phases, such as in rocks, pressure can be discontinuous as shown in the first part of this work. Therefore a complementary approach to the modification of the thermodynamic potentials under pressure variations would be a use of the already existing formulations (Gibbs, 1906) only requiring the removal of the constraint of constant pressure (Tajčmanová et al., 2014). In fact, the Gibbs energy as a function of pressure is more convenient for a system under pressure variations than Helmholtz energy because it requires no modification of the current input data in petrology modelling (i.e. internally consistent thermodynamic datasets and activity models). The Gibbs energy can be then minimized to consider phase relationships under pressure gradients, if it is appropriately constrained (Vrijmoed and Podladchikov, 2014).

3.3. Equilibrium versus stationary state

In petrology, three distinct views for quantification of a microstructure are used – an equilibrium view, a stationary (steady) state view and a sluggish kinetics (thermal closure) view. An equilibrium view builds a basis of thermobarometric methods (i.e. no macroscopic mass fluxes), assuming that the equilibrium relationships are preserved during cooling. The steady-state view has its application in diffusion-controlled microstructures and geospeedometry and assumes diffusion-controlled closure during cooling. For selecting appropriate thermodynamic formulations for systems with pressure variations, it is essential to highlight the differences between equilibrium and steady state, i.e. for states above the closure temperature of the system during cooling.

A system being in thermodynamic equilibrium in the sense of Gibbs (1906) is characterized by homogeneity of the thermodynamic potentials (i.e. pressure, temperature and chemical potentials are constant; e.g. Callen, 1985; Kondepudi and Prigogine, 1998). If a heterogeneous system is considered, such as when several minerals occur together in a rock, it can be split into several local domains in which P, T and μ are well defined (shown as boxes in Fig. 7). Such a domain is then referred to as being in local thermodynamic equilibrium. Thermodynamic equilibrium is represented by the absence of macroscopic fluxes, zero entropy production and the Gibbs energy is at a minimum (Fig. 7a). A special case of thermodynamic equilibrium is equilibrium under external forces (e.g. a fluid under gravity; Gibbs, 1906; Landau and Lifshitz, 1987). Such an equilibrium is characterized by gradients of thermodynamic potentials (e.g. pressure) while keeping zero macroscopic fluxes (Fig. 7b; Landau and Lifshitz, 1987, p. 236). To account for the gradients requires an independent mechanical model complementary to the thermodynamic treatment of such equilibrium. Consider as an example a glass of water in a gravity field. The pressure will change linearly with depth but this does not mean that the glass of water cannot be in thermodynamic equilibrium. The equilibrium under external forces is useful for treating solids, where for mechanical reasons variations in pressure are expected under the assumption that viscous relaxation is slow.

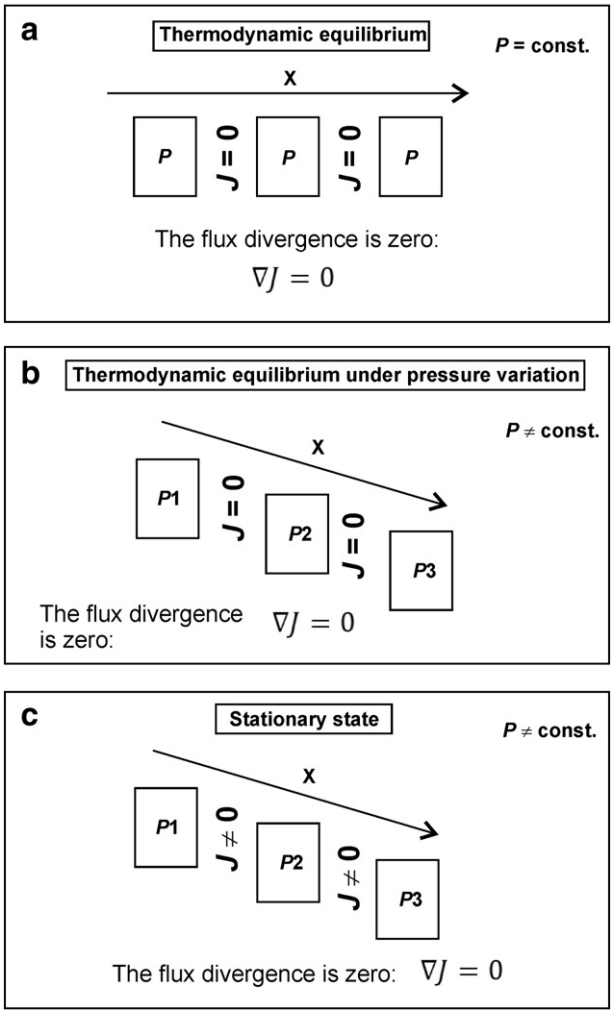

Fig. 7. The difference among a) classical thermodynamic equilibrium; b) equilibrium under external forces (pressure variation) and c) stationary state for a system with pressure variation. Each box represents a local equilibrium domain with defined P, T and μ. Thermodynamic equilibrium is achieved when entropy production is zero. The necessary condition for this equilibrium is that the local fluxes (J) and their divergence are zero. The stationary state is characterized by zero flux divergence but non-zero macroscopic fluxes between boxes.

Conversely, a system can be in a stationary state (i.e. not evolving with time) while gradients of thermodynamic potentials are maintained (e.g. pressure, temperature). The difference between an equilibrium state and a stationary state is defined in terms of whether entropy production is involved. In a stationary state the divergence of the fluxes is zero, but not the fluxes between the locally equilibrated domains themselves (Fig. 7c). This results in non-zero entropy production (e.g. Moore, 1962).

The important step in understanding the phase relationships and behaviour in systems under grain-scale pressure variation is to focus on equilibrium thermodynamic formulations. The petrology relevance then lies in the thermobarometric methods and phase equilibria modelling that can then be applied.

3.4. Equilibrium under pressure gradients

Several specialised analyses of species segregation in biotechnology, chemical engineering and for deep-oil reservoirs use an equilibrium formulation for calculating compositional gradients either under external forces such as gravity which may be responsible for the maintenance of a pressure gradient or due to an osmotic pressure difference through a semipermeable membrane (Espósito et al., 2000; Gibbs, 1906; Landau and Lifshitz, 1987; Martins et al., 2005; Miller, 1956; Müller and Weiss, 2012; Savenko and Dijkstra, 2004; Wensink and Lekkerkerker, 2004; Young et al., 1954). In these analyses, the principles of energy, momentum and mass conservation are followed. A geologically relevant application of the aforementioned approach is the calculation of mineral equilibria under mechanically-imposed grain-scale pressure variations as considered in this review.

Similarly to the centrifugation effects mentioned above, a mechanically–maintained pressure variation is likely to cause a redistribution of components in minerals, with higher density minerals and mineral compositions developing towards the higher pressure. Therefore, a chemical zonation can occur as a result of variation in pressure under thermodynamic equilibrium if the pressure gradient is maintained. The classical petrology view focuses only on spatial chemical variations among mineral phases under the assumption that rocks are weak and that pressure is uniform among grains (Fig. 8a). Then these chemical variations are assumed to reflect variation in chemical potential and the zoned minerals suggest that chemical equilibrium was not attained (Fig. 8a). Such a system may then be treated as a (preserved) stationary state in order to be quantified (e.g. Fisher, 1973; Joesten, 1977; Nishiyama, 1983). Moreover, the zoned microstructure can be used as a geospeedometer if assumed to be "frozen" due to sluggish kinetics (e.g. Lasaga, 1998). On the contrary, spatial variations in pressure, at mechanical equilibrium, lead to a chemical zoning in minerals (Fig. 8b). Such a system can be at thermodynamic equilibrium with the chemical variation, as long as the pressure variation is maintained.

A geologically relevant example of such a thermodynamic equilibrium under external forces has been recently presented by Tajčmanová et al. (2014). In their work, the apparent disequilibrium chemical zoning of plagioclase was explained using equilibrium thermodynamics under an externally imposed pressure gradient between kyanite and the surrounding low-pressure matrix (Fig. 8c). Such an explanation assumes diffusional fluxes to be zero across the chemically zoned plagioclase grain when the equilibrium was established at high temperature. The thermodynamic treatment at zero flux requires an appropriate use of chemical potential. The unconventional barometer based on the chemical zonation proposed by Tajčmanová et al. (2014) predicts 0.8 GPa of pressure difference across the plagioclase grain, between the kyanite and the low pressure matrix, for the example considered. The unconventional barometer is the result of an equilibrium thermodynamics approach independent of rheological or kinetic parameters.

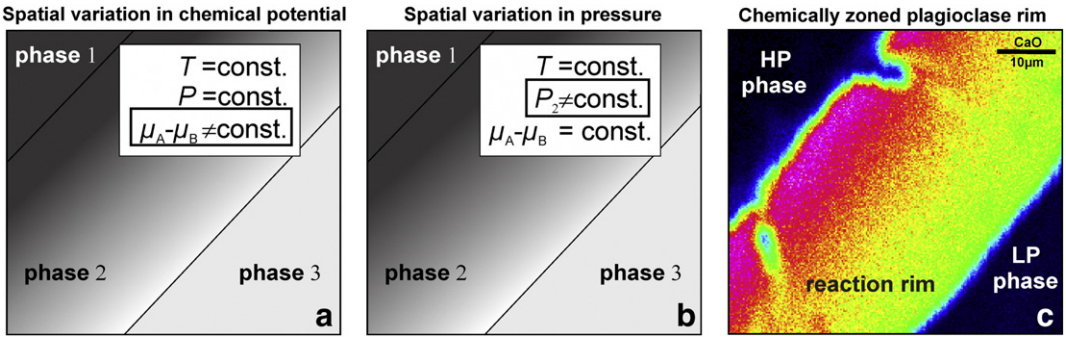

Fig. 8. a) Spatial chemical variation (gray-shading) is assumed to reflect a variation in chemical potential difference between component A and B. Such an interpretation characterizes disequilibrium. b) Chemical zoning reflecting a spatial variation in pressure as a result of mechanical equilibrium. c) A plagioclase reaction rim between high-pressure (HP) and low-pressure (LP) phases (modified after Tajčmanová et al., 2011).

In order to see the effect of an externally-imposed pressure gradient on the chemical zoning in a mineral, a binary example of diffusion transfer of albite and anorthite components in plagioclase associated with kyanite (as in Fig. 8c) is considered. The approach is comparable to density redistribution due to pressure controlled mass transfer at centrifugation equilibrium described in the works mentioned earlier. The example is represented by a series of snapshots with a final achievement of a equilibrium state. The reason for the pressure gradient as well as the modification of chemical potential is beyond the scope of this review with details to be found in Tajčmanová et al. (2014).

In a binary system, the amount of one of the two components is independent. For the derivation below, *A* is assumed to be the independent chemical component. See Table 1 for a complete list of symbols. The various forms of chemical potential (molar and mass, respectively) for component *A* in a phase are (e.g. Cemič, 2005; Powell, 1978):

$$\begin{cases} \overline{\mu}^A = \overline{g} + \left(1-\overline{c}^A\right)\dfrac{\partial \overline{g}}{\partial \overline{c}^A} = \overline{\mu}_0^A(T,P) + RT\ln\left(\overline{a}^A\right) \approx \underbrace{\overline{\mu}_0^A(T,P) + RT\ln\left(\overline{c}^A\right)}_{ideal} & (molar) \\ \mu^A = g + \left(1-c^A\right)\dfrac{\partial g}{\partial c^A} = \mu_0^A(T,P) + \dfrac{RT\ln\left(a^A\right)}{M^A} \approx \underbrace{\mu_0^A(T,P) + \dfrac{RT\ln\left(\overline{c}^A\right)}{M^A}}_{ideal} & (mass) \end{cases} \tag{23}$$

where *a* is activity (effective concentration) of an end-member or a component, *c* is chemical composition of an end-member or a component (for details see e.g. Cemič, 2005). The bars are used for molar quantities. Note that apart from the units, the only difference between the molar and mass formulation is the division of the logarithmic term by molar mass (i.e. M^A for component A). The approximate equality in Eq. (23) is for an ideal model.

The composition-independent part of the chemical potential (μ_0) is a function of pressure and temperature but not composition. If equilibrium at constant pressure and temperature is assumed across a rock sample, then μ_0 is constant spatially. However, the *P* dependence of μ_0 becomes important for chemical redistribution in mineral grains with externally imposed spatial pressure variation (as in Fig. 8b) because the volume of minerals (and therefore μ_0) change with pressure. When mass transfer is taken into account, mass conservation requires (de Groot and Mazur, 1962; p. 340):

$$\rho\frac{dc^A}{dt} = -\nabla J^A \tag{24}$$

where c^A is the concentration (mass fraction) of the component *A* in the solution and J^A is the mass flux of that component. The commonly used expression for the flux (c.f. Nauman and He, 2001) which is compatible with zero gradient of chemical potential at equilibrium is:

$$J^A = -\frac{\rho}{RT}DM^A\overline{c}^A\nabla\mu^A \tag{25}$$

The expression is multiplied by $\frac{\rho}{RT}$ in order to be in agreement with classical Fickian diffusion. The diffusion coefficient (D in m^2/s) is then treated as a linear proportionality factor between flux of mass and chemical potential gradient. The diffusion coefficient will affect only the time needed for the system to reach equilibrium so its absolute value is not important for controlling the chemical zoning at equilibrium. The key idea is that the pressure dependence of chemical potential (Eq. (23)) is involved in the diffusion flux equation (Eq. (25)):

$$J^A = -\frac{\rho}{RT}DM^A\overline{c}^A\left(\frac{\partial\mu^A}{\partial\overline{c}^A}\nabla\overline{c}^A + \frac{\partial\mu^A}{\partial P}\nabla P\right) \tag{26}$$

Therefore, for a binary system with components *A* and *B* and following the appropriate definition of chemical potential for systems with pressure variation, the fluxes for the case of a solid showing ideal mixing are:

$$\begin{aligned} J^A &= -\rho D\left(\nabla\overline{c}^A + \overline{c}^A M^A\frac{\partial\mu_0^A}{\partial P}\frac{\nabla P}{RT}\right) \\ J^B &= -\rho D\left(\nabla\overline{c}^B + \overline{c}^B M^B\frac{\partial\mu_0^B}{\partial P}\frac{\nabla P}{RT}\right) \end{aligned} \tag{27}$$

The derivative of the standard partial Gibbs energy (μ_0) with respect to pressure multiplied by the molar mass (M^A) is equal to the partial molar volume. Therefore, Eq. (27) become

$$\begin{aligned} J^A &= -\rho D\left(\nabla\overline{c}^A + \overline{c}^A\frac{\overline{V}^A\nabla P}{RT}\right) \\ J^B &= -\rho D\left(\nabla\overline{c}^B + \overline{c}^B\frac{\overline{V}^B\nabla P}{RT}\right) \end{aligned} \tag{28}$$

where $\overline{V}$ is a molar volume of an end member. In chemical equilibrium, these fluxes and their sum must be equal to zero (see stationary versus equilibrium section). However, the equilibrium relation for a system under pressure variations leads to an inconsistency.

$$0 = J^A + J^B = -\frac{\rho D}{RT}\left(\overline{c}^A\overline{V}^A + \overline{c}^B\overline{V}^B\right)\nabla P \neq 0 \tag{29}$$

The inconsistency points to the conceptual error in Eq. (25). The gradients of chemical potentials under pressure variations are not zero, in equilibrium, only the gradient of their difference is equal to zero Tajčmanová et al. (2014). This requirement must be implemented into the flux equation (Eq. (25)) so that the sum of the fluxes is zero in equilibrium. Therefore, the expression for flux compatible with such an equilibrium, is:

$$J^A = -\frac{\rho}{RT} D \bar{c}^A \bar{c}^B \frac{M^A M^B}{M^A \bar{c}^A + M^B \bar{c}^B} \nabla\left(\mu^A - \mu^B\right). \tag{30}$$

In addition, there is also an inconsistency related to the assumption of equality of mass and molar concentrations. In fact, Nauman and He (2001) also reported that the assumption of equal molar counter-diffusion can be grossly incorrect, for example, in polymers systems. In petrology, due to similarity of molar volume for common minerals, the molar reference frame is assumed to be a reasonable approximation (e.g. Loomis, 1978). However, this approximation cannot be generally applied as shown below. Careful treatment of the mass and molar concentrations has been described for instance in de Groot and Mazur (1962), McLellan (1980), Thomas (1993) and Kuiken (1994). For example, in the case of an ideal binary system, the above flux equation (Eq. (30)) after the substitution of Eq. (23) has different mass versus mole forms under a pressure gradient:

$$\begin{cases} J^A = -\rho D\left(\nabla \bar{c}^A + \dfrac{\nabla P}{RT}\left(\overline{V}^A - \overline{V}^B\right)\bar{c}^A \bar{c}^B \right) & (molar) \\ J^A = -\rho D\left(\nabla \bar{c}^A + \dfrac{\nabla P}{RT}\left(V^A - V^B\right)\bar{c}^A \bar{c}^B \dfrac{M^A M^B}{M^A \bar{c}^A + M^B \bar{c}^B} \right) & (mass) \end{cases} \tag{31}$$

The relatively complex multiplier $\left(\frac{M^A M^B}{M^A \bar{c}^A + M^B \bar{c}^B}\right)$ in front of the gradient of the chemical potential difference in Eq. (30) was chosen to be consistent with the Fickian behavior. At constant pressure, substitution of the flux expression into the mass balance equation Eq. (24) and assuming constant density and equality of molar and mass concentrations yields the classical Fickian diffusion limit:

$$\frac{dc^A}{dt} = \nabla\left(D \nabla \bar{c}^A\right) \tag{32}$$

At equilibrium under pressure gradients:

$$\begin{cases} \dfrac{1}{\bar{c}^A \bar{c}^B} \nabla \bar{c}^A = -\left(\overline{V}^A - \overline{V}^B\right)\dfrac{\nabla P}{RT} & (molar) \\ \dfrac{M^A \bar{c}^A + M^B \bar{c}^B}{M^A M^B \bar{c}^A \bar{c}^B} \nabla \bar{c}^A = -\left(V^A - V^B\right)\dfrac{\nabla P}{RT} = -\left(\dfrac{1}{\rho_A} - \dfrac{1}{\rho_B}\right)\dfrac{\nabla P}{RT} & (mass) \end{cases} \tag{33}$$

Eq. (33) shows that, in equilibrium, gradients in composition are balanced by gradients in pressure. The coefficient in front of the compositional gradient (left hand side of the Eq. (33)) is always positive. The trend of compositional zoning is then controlled by the sign of the molar volume and density difference in molar and mass formulation, respectively. Therefore the prediction of the zoning trend as a response to an externally imposed pressure gradient may lead to different results depending on which of the two formulations is used. Interestingly, the sign of the molar volume and the density difference can be opposite (e.g. Fig. 9). Furthermore, Fig. 9 shows a flip in molar volume of albite and anorthite at 15 kbar pointing to a dependence on the absolute *P-T* conditions as well. Therefore, the use of appropriate units in the equations for fluxes for a system under pressure variation is essential. The plagioclase example shows that even though the molar volumes are almost identical, the conversion to mass units leads to radical changes. Such a difference between molar volume and mass can also be found for the grossular and pyrope end-members in garnet.

To show the consequences of the above mentioned approach, a simple numerical simulation is presented. Eqs. (24) and (30) are combined in order to solve the composition evolution of a solution over time. In the case of a binary mixture, such as plagioclase, $A = Ab$ (albite) and $B = An$ (anorthite). This means that only one diffusion equation has to be solved to describe the evolution of the system. In order to solve the

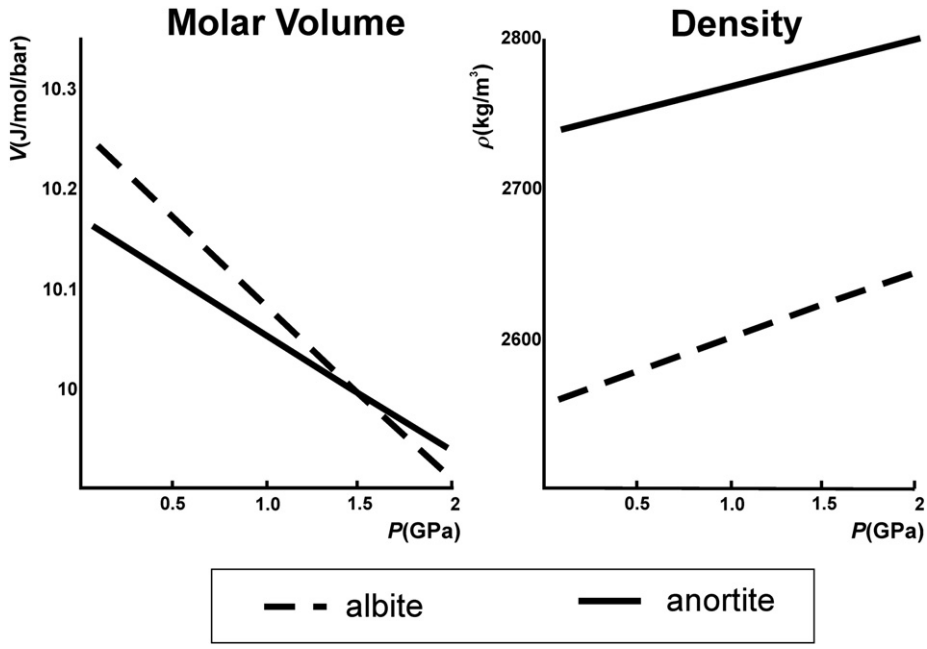

Fig. 9. a) Molar volumes (J/mol/bar) and b) density (kg/m^3) of albite and anortite end members (taken Holland and Powell, 1998). The molar volumes of albite and anorthite are approximately the same. On the contrary, when converted to mass (kg), a significant difference (about 6%) between the two end members is obtained. Such a magnitude is important when involved in the equation for fluxes (Eq. (30)).

diffusion equation, a 1-d explicit finite difference numerical scheme is employed (e.g. Anderson, 1995). An externally imposed pressure profile predicted by the unconventional barometer of Tajčmanová et al. (2014) and constant temperature throughout the plagioclase is assumed (Fig. 10). No flux of material at the left boundary and fixed composition at the right boundary are taken as boundary conditions. One compositional variable (c^{Ab}) is explicitly solved for both models as constrained from plagioclase composition (i.e. $c^{Ab} + c^{An} = 1$). The chemical potentials are calculated using the thermodynamic database of Holland and Powell (1998 updated 2003) and the solid solution of plagioclase as in (Fuhrman and Lindsley, 1988). Diffusion coefficient ($D = 10^{-21}$) was chosen to be close to the real value (Yund, 1986) at temperature of 800 °C.

If pressure variation is imposed in an initially chemically homogeneous plagioclase grain, there is a driving force for diffusion (Fig. 10a,b). This is due to the functional dependence of the chemical potentials on pressure shown earlier. The non-zero chemical potential difference leads to the development of a diffusion flux (at t = 13 kyr) which is responsible for creating a chemically zoned profile in plagioclase (Fig. 10a). At a given time ($t = t_{eq} >> 13$ kyr), chemical diffusion brings the system to the equilibrium state (Fig. 10c,d). Under these conditions, diffusion fluxes are zero but the plagioclase grain is not homogenous in composition. If the pressure gradient had been removed then, the diffusion process would have started to operate again, driven by concentration gradients.

4. Concluding remarks

The metamorphic rocks produced in orogenic belts are a key to understanding the processes operating in the Earth's interior. Pressure is an important quantity that controls metamorphic reactions. Pressure estimates also provide constraints on geodynamic reconstructions. Depth estimates made with the lithostatic formula ($P = \rho g h$) are incorrect if the thermodynamic pressure estimate deviates significantly from the lithostatic pressure (>20%, e.g. Schmalholz et al., 2014b). Such a deviation can be evaluated, for instance, by careful comparison of metamorphic records with structural ones (Pleuger and Podladchikov, 2014). Therefore, in order to generate physically consistent geodynamic reconstructions and to understand crustal/lithospheric deformation, it is essential to have physically consistent interpretations of petrographic observations. New observations show that mechanically maintained pressure variations are significant (~1 GPa) even on a micrometre-scale. In this review, it has also been shown that it is mechanically feasible to maintain such pressure variations at geological time scales. However, such pressure variations have not been properly considered in conventional petrology quantification approaches. When attempting

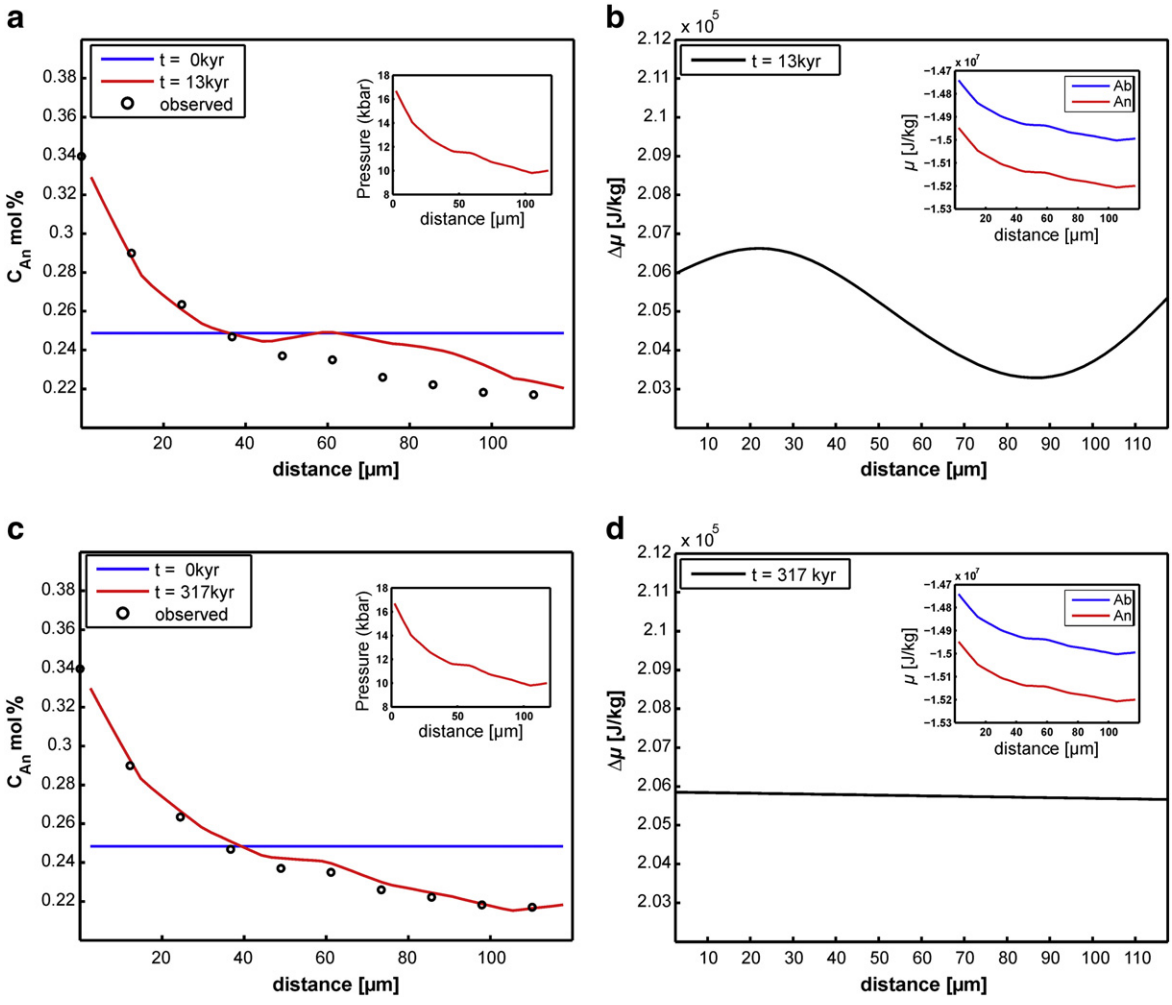

Fig. 10. Results of the numerical model illustrating the development of equilibrium in plagioclase under an externally imposed pressure gradient. The numerical setup follows the results of the "unconventional" barometer of Tajčmanová et al. (2014). a) Chemical composition of plagioclase as a function of distance. Black dots represent measured plagioclase compositions across the rim (Tajčmanová et al., 2011, 2014). The blue profile is the initial profile for t = 0. The red profile is after ca 13 kyr. The pressure profile across the grain is shown on the inset. b) Chemical potential difference ($\Delta\mu = \mu^{Ab} - \mu^{An}$) across plagioclase for the time 13 kyr. The chemical potentials are plotted separately in the inset. The chemical potentials are calculated at temperature of 800 °C. c) As in (a) for t = teq ≈ 317 kyr. At teq the diffusion has stopped and the system reached equilibrium. d) As in (b) but for t = teq ≈ 317 kyr. Note that the chemical potential difference is constant in space, but the individual chemical potentials are not. Abbreviations: Ab = albite; An = anorthite.

to apply currently available thermodynamic methods to describe and interpret rocks that involve grain-scale pressure variations, petrologists face fundamental problems. For example, the UHP observations such as coesite in Dora Maira (Chopin, 1984) need not necessarily correspond to large depths. In fact, they can be a result of a local UHP pressure perturbation in a rock mass (e.g. Vrijmoed et al., 2009). Such an interpretation is supported by models of Schmalholz et al. (2014b). They show that crustal rocks can reach UHP conditions (2.5-3 GPa) even under middle crustal conditions. If such a local pressure perturbation was converted to depth, the error in a depth estimate would be bigger than a typical thickness of the whole continental crust (Fig. 11). Therefore, in the absence of an appropriate quantification approach, errors from the *P-T* estimates can then propagate to geodynamic models and hence can confuse our understanding of the global processes in Earth's crust.

4.1. The quantification dilemma

Most effort in quantifying consideration of systems with large volumetric changes during metamorphic reactions has focused mostly on the contribution of nonhydrostatic stress to the energetics (e.g. Dahlen, 1992; Fletcher and Merino, 2001; Kamb, 1961; Wheeler, 1987, 2014). However, the direct contribution of nonhydrostatic stress to the internal energy is likely to be small in comparison with how significant the effect of pressure variations on results from metamorphic phase equilibria modelling may be (Connolly, 2009).

Unfortunately, as shown in this work, none of the nonhydrostatic theories for solid-solid equilibrium have been fully proved by experiment or natural observations so far. A question is whether it is really unavoidable to apply nonhydrostatic thermodynamics for nonhydrostatically stressed solids. Interestingly, an alternative explanation of the coesite/quartz experiment of Hirth and Tullis (1994) based on heterogeneous pressure distribution in the grain scale was proposed by Moulas et al. (2013); see also Schmalholz and Podladchikov (2014). Moulas et al. (2013) suggested that the newly grown coesite in the Hirth and Tullis's experiments grew under low differential stress. By having small differential stress, coesite crystals growing in faces oriented perpendicular to $\sigma 1$ have mean stress close to the value of $\sigma 1$ due to force balance (see Fig. 5 in Moulas et al., 2013). In fact, crystals having small differential stress will have lower energy and therefore are energetically favourable. Therefore, the hydrostatic approach seems to be more plausible solution rather than the complex nonhydrostatic theories. This suggests the classical approach of Gibbs (1906) to be applicable also in nonhydrostatic solids.

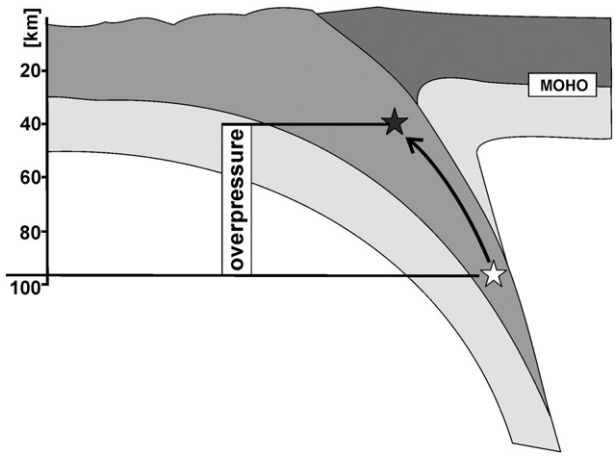

Fig. 11. Sketch of a subduction setting illustrating the error related to the wrong interpretation of UHP observations. See the work of Schmalholz et al. (2014b) for more specific example on the tectonic interpretation of the Dora Maira UHP occurrence.

Most of the previous equilibrium quantification approaches aim to combine both processes, mechanical and chemical, into one equation. This seems to be unnecessarily difficult especially for rocks with solid solutions. The new direction, the application of equilibrium under a pressure gradient, introduced by Tajčmanová et al. (2014) suggests splitting the problem into two parts. First, a rigorous mechanical model predicting the pressure variation should be made independently. Then a chemical equilibrium formulation which couples pressure and density is superimposed on it. The equilibrium under pressure variations is also independent of the hydrostatic and nonhydrostatic dilemma. Similarly to pressure variation in a glass of water or in the atmosphere, pressure gradients can be treated as a hydrostatic problem. The next step in the quantification procedure is to develop a methodology for minimizing Gibbs energy involving constraints that allow calculation of phase equilibrium diagrams for systems with heterogeneous pressures (Vrijmoed and Podladchikov, 2014).

4.2. Future work

The recent analytical and theoretical advances imply that petrographic observations should be reconsidered in the light of pressure variations. Possible spatial pressure gradients must be carefully documented. This, on the one hand, opens new horizons in metamorphic petrology but, on the other hand, it can bring some uncertainties into the currently common assumptions, such as pressure-to-depth conversion. In fact, if all observations are treated only by conventional methods based on the constant pressure assumption, the interpretations may not represent the appropriate mechanism explaining the microstructure. Considering pressure variations as the other possible interpretation (for details see Tajčmanová et al., 2014), an alternative model for the development of petrographic observations can be inferred. Furthermore, such variations can be mechanically maintained over several million years. Natural observations most probably reflect a combination of the two end-members. In fact, in cases where the conventional approach gives physically feasible results with respect to a regional geology setting, it can be assumed as an appropriate solution. However, in cases where there is a clear evidence of a spatial pressure variation just simply based on the petrographic observation of high-pressure and low-pressure phases in one thin-section, an alternative approach should be considered. Moreover, we can have observations where the originally maintained pressure variation was mechanically removed during the geological evolution of the rock and the classical diffusion takes place (Moulas et al., 2015). Therefore, both quantification directions need to be taken into account in petrology interpretations. The approach that allows for full understanding of the observations is then the most suitable one. Moreover, ignoring the presence of pressure variations in petrology quantification may also influence directly the interpretations not only in UHP terrains but also in regional metamorphic terrains. For example, it is commonly interpreted that preservation of key phases outside their stability fields is due to sluggish kinetics or reaction overstepping (Carlson, 2002; Kelly et al., 2013; Pattison et al., 2011). In fact, mechanically maintained pressure variations can be suggested as an alternative explanation. Such variations may be responsible for the preservation of the phases apparently outside their stability field.

The observed variations in metamorphic grades due to the pressure variation in the same depth would not then be suitable for pressure-to-depth conversion. Ignoring such pressure variations in petrological analysis can lead to large errors in depth estimates (Fig. 11). However, they might provide important indications on differential stress and strength variations in a rock. Therefore, the future research in this direction may focus on how the pressure variation can be used to constrain rheology properties directly from natural microstructures. The UHP observations would not then lose their importance but might play a different role in geodynamic reconstructions (Yang et al., 2014).

Acknowledgements

This work was supported by MADE-IN-EARTH ERC starting grant (n. 335577). Yuri Podladchikov and Roger Powell are acknowledged for helpful discussions and for critical reading of earlier version of the manuscript. This work benefited from detailed reviews by T. Gerya and S. Schmalholz. Editorial assistance by M. Scambelluri is also acknowledged.

References

Andersen, T.B., Mair, K., Austrheim, H., Podladchikov, Y.Y., Vrijmoed, J.C., 2008. Stress release in exhumed intermediate and deep earthquakes determined from ultramafic pseudotachylyte. Geology 36, 995–998.
Anderson, J.D., 1995. Computational fluid dynamics: The basics with applications. McGraw-Hill. (547 pp.).
Ashworth, J., Birdi, J., 1990. Diffusion modelling of coronas around olivine in an open system. Geochimica et Cosmochimica Acta 54, 2389–2401.
Bailey, E.H., Irwin, W.P., Jones, D.L., 1964. Franciscan and related rocks, and their significance in the geology of western California. California Division of Mines and Geology Bulletin 183 (177 pp.).
Brace, W.F., Ernst, W.G., Kallberg, R.W., 1970. An experimental study of tectonic overpressure in Franciscan rocks. Geological Society of America Bulletin 81, 1325–1338.
Burg, J.P., Gerya, T.V., 2005. The role of viscous heating in Barrovian metamorphism of collisional orogens: thermomechanical models and application to the Lepontine Dome in the Central Alps. Journal of Metamorphic Geology 23, 75–95.
Callen, H.B., 1985. Thermodynamics and an introduction to thermostatistics. 2nd edition. Wiley (493 pp.).
Carlson, W.D., 2002. Scales of disequilibrium and rates of equilibration during metamorphism. American Mineralogist 87, 185–204.
Castier, M., Tavares, F.W., 2005. Centrifugation equilibrium of natural gas. Chemical Engineering Science 60, 2927–2935.
Cemič, L., 2005. Thermodynamics in mineral sciences. Springer (386 pp.).
Chopin, C., 1984. Coesite and pure pyrope in high-grade blueschists of the Western Alps: a first record and some consequences. Contributions to Mineralogy and Petrology 86, 107–118.
Connolly, J.A.D., 2009. The geodynamic equation of state: What and how. Geochemistry, Geophysics, Geosystems 10, Q10014.
Cruden, A.R., 1990. Flow and fabric development during the diapiric rise of magma. Journal of Geology 98, 681–698.
Dabrowski, M., Powell, R., Podladchikov, Y., 2015. Viscous relaxation of grain-scale pressure variations. Journal of Metamorphic Geology (in press).
Dahlen, F.A., 1992. Metamorphism of nonhydrostatically stressed rocks. American Journal of Science 292, 184–198.
De Capitani, C., Petrakakis, K., 2010. The computation of equilibrium assemblage diagrams with Theriak/Domino software. American Mineralogist 95, 1006–1016.
De Groot, S.R., Mazur, P., 1962. Non–Equilibrium Thermodynamics. Amsterdam, North–Holland Pub. Co., New York, Interscience Publishers, (510 pp.).
Dimanov, A., Dresen, G., Wirth, R., 2000. The effect of melt distribution on the rheology of plagioclase rocks. Tectonophysics 328, 307–327.
Enami, M., Nishiyama, T., Mouri, T., 2007. Laser Raman microspectrometry of metamorphic quartz: A simple method for comparison of metamorphic pressures. American Mineralogist 92, 1303–1315.
Espósito, R.O., Castier, M., Tavares, F.W., 2000. Calculations of thermodynamic equilibrium in systems subject to gravitational fields. Chemical Engineering Science 55, 3495–3504.
Etheridge, M.A., 1983. Differential stress magnitudes during regional deformation and metamorphism: Upper bound imposed by tensile fracturing. Geology 11, 231–234.
Ferguson, C.C., Harvey, P.K., 1980. Porphyroblasts and "crystallization force": Some textural criteria: Discussion. Geological Society of America Bulletin 83, 3839–3840.
Feynman, R., 1967. The character of physical law. MIT Press. (192 pp.).
Fisher, G.W., 1973. Nonequilibrium thermodynamics as a model for diffusion-controlled metamorphic processes. American Journal of Science 273, 897–924.
Fletcher, R.C., 1982. Coupling of diffusional mass transport and deformation in a tight rock. Tectonophysics 83, 275–291.
Fletcher, R.C., Merino, E., 2001. Mineral growth in rocks: kinetic-rheological models of replacement, vein formation, and syntectonic crystallization. Geochimica et Cosmochimica Acta 65, 3733–3748.
Fuhrman, M.L., Lindsley, D.H., 1988. Ternary feldspar modeling and thermometry. American Mineralogist 73, 201–215.
Gerya, T.V., Perchuk, L.L., Burg, J.-P., 2008. Transient hot channels: Perpetrating and regurgitating ultrahigh-pressure, high-temperature crust-mantle associations in collision belts. Lithos 103, 236–256.
Gibbs, J.W., 1906. The scientific papers: Thermodynamics. Longmans, Green and co, London (434 pp.).
Green, H.W., 2005. Psychology of a changing paradigm: 40+ years of high-pressure metamorphism. International Geology Review 47, 439–456.
Grinfeld, M., 1991. Thermodynamic methods in the theory of heterogeneous systems, Harlow, Longman Scientific & Technical (399 pp.).
Hillert, M., 2007. Phase equilibria, phase diagrams and phase transfromations: Their thermodynamic basis. Cambridge University Press (510 pp.).
Hirth, G., Tullis, J., 1994. The brittle-plastic transition in experimentally deformed quartz aggregates. Journal of Geophysical Research, Solid Earth 99, 11731–11747.
Holland, T.J.B., Powell, R., 1998. An internally consistent thermodynamic data set for phases of petrological interest. Journal of Metamorphic Geology 16, 309–343.
Howell, D., 2012. Strain-induced birefringence in natural diamond: a review. European Journal of Mineralogy 24, 575–585.
Howell, D., Wood, I.G., Dobson, D.P., Jones, A.P., Nasdala, L., Harris, J.W., 2010. Quantifying strain birefringence halos around inclusions in diamond. Contributions to Mineralogy and Petrology 160, 705–717.
Ji, S., Wang, Q., 2011. Interfacial friction induced pressure and implications for the formation and preservation of intergranular coesite in metamorphic rocks. Journal of Structural Geology 33, 107–113.
Joesten, R., 1977. Evolution of mineral assemblage zoning in diffusion metasomatism. Geochimica et Cosmochimica Acta 41, 649–670.
Kamb, W.B., 1961. The thermodynamic theory of nonhydrostatically stressed solids. Journal of Geophysical Research 66, 259–271.
Kelly, E.D., Carlson, W.D., Ketcham, R.A., 2013. Magnitudes of departures from equilibrium during regional metamorphism of porphyroblastic rocks. Journal of Metamorphic Geology 31, 981–1002.
Kondepudi, D., Prigogine, I., 1998. Modern thermodynamics: From heat engines to dissipative structures. Wiley (508 pp.).
Kuiken, G.D.C., 1994. Thermodynamics of irreversible processes: Applications to diffusion and rheology. Wiley (Chapter 6, 458 pp.).
Landau, L.D., Lifshitz, E.M., 1987. 2nd edition. Fluid Mechanics vol. 6. Butterworth Heinemann, Oxford, UK (539 pp.).
Lasaga, A., 1998. Kinetic theory in the earth sciences. Princeton University Press, New Jersey, USA (811 pp).
Lewis, G.N., Randall, M., 1923. Thermodynamics and the free energy of chemical substances. McGraw-Hill. (653 pp.).
Li, Z.H., Gerya, T.V., Burg, J.P., 2010. Influence of tectonic overpressure on P–T paths of HP–UHP rocks in continental collision zones: thermomechanical modelling. Journal of Metamorphic Geology 28, 227–247.
Liou, J.G., Zhang, R.Y., 1996. Occurrence of intragranular coesite in ultrahigh-P rocks from the Sulu region, eastern China: implications for lack of fluid during exhumation. American Mineralogist 81, 1217–1221.
Liu, M., Kerschhofer, L., Mosenfelder, J.L., Rubie, D.C., 1998. The effect of strain energy on growth rates during the olivine-spinel transformation and implications for olivine metastability in subducting slabs. Journal of Geophysical Research, Solid Earth 103, 23897–23909.
Loomis, T.P., 1978. Multicomponent diffusion in garnet: I. formulation of isothermal models. American Journal of Science 278, 1099–1118.
Mancktelow, N.S., 1995. Nonlithostatic pressure during sediment subduction and the development and exhumation of high pressure metamorphic rocks. Journal of Geophysical Research 100, 571–583.
Mancktelow, N.S., 2008. Tectonic pressure: Theoretical concepts and modelled examples. Lithos 103, 149–177.
Martins, L.S.F., Tavares, F.W., Castier, M., 2005. Centrifugation equilibrium for spheres and spherocylinders. Journal of Colloid and Interface Science 281, 360–367.
McLellan, A.G., 1980. The classical thermodynamics of deformable materials. Cambridge monographs on physics. Cambridge University Press (358 pp.).
Milke, R., Abart, R., Kunze, K., Koch-Mueller, M., Schmid, D., Ulmer, P., 2009. Matrix rheology effects on reaction rim growth I: evidence from orthopyroxene rim growth experiments. Journal of Metamorphic Geology 27, 71–82.
Miller, D.G., 1956. Thermodynamic theory of irreversible processes. II. Sedimentation equilibrium of fluids in gravitational and centrifugal fields. American Journal of Physics 24, 555–561.
Moghadam, R.H., Trepmann, C.A., Stöckhert, B., Renner, J., 2010. Rheology of synthetic omphacite aggregates at high pressure and high temperature. Journal of Petrology 51, 921–945.
Molnar, P., Lyon-Caen, H., 1988. Some simple physical aspects of the support, structure, and evolution of mountain belts. Geological Society of America, Special Paper 218, 179–208.
Moore, W.J., 1962. Physical chemistry. 4th ed. Longmans, Green, and CO (977 pp.).
Morris, S.J.S., 2002. Coupling of interface kinetics and transformation-induced strain during pressure-induced solid–solid phase changes. Journal of the Mechanics and Physics of Solids 50, 1363–1395.
Morris, S.J.S., 2014. Kinematics and thermodynamics of a growing rim of high-pressure phase. Physics of the Earth and Planetary Interiors 228, 127–143.
Mosenfelder, J.L., Connolly, J.A.D., Rubie, D.C., Liu, M., 2000. Strength of (Mg, Fe)2SiO4 wadsleyite determined by relaxation of transformation stress. Physics of the Earth and Planetary Interiors 120, 63–78.
Moulas, E., Podladchikov, Y.Y., Aranovich, L.Y., Kostopoulos, D., 2013. The problem of depth in geology: When pressure does not translate into depth. Petrology 21, 527–538.
Moulas, E., Burg, J.-P., Podladchikov, Y., 2014. Stress field associated with elliptical inclusions in a deforming matrix: Mathematical model and implications for tectonic overpressure in the lithosphere, Tectonophysics 631 pp. 37–49.
Moulas, E., Tajčmanová, L., Vrijmoed, J., Podladchikov, Y., 2015. Diffusion and thermodynamic equilibrium under pressure variations. Geophysical Research Abstracts 17.
Müller, I., Weiss, W., 2012. Thermodynamics of irreversible processes—past and present. The European Physical Journal H 37, 139–236.
Nasdala, L., Hofmeister, W., Harris, J.W., Glinnemann, J., 2005. Growth zoning and strain patterns inside diamond crystals as revealed by Raman maps. American Mineralogist 90, 745–748.
Nauman, E.B., He, D.Q., 2001. Nonlinear diffusion and phase separation. Chemical Engineering Science 56, 1999–2018.

Nishiyama, T., 1983. Steady diffusion model for olivine-plagioclase corona growth. Geochimica et Cosmochimica Acta 47, 283–294.
Parkinson, C.D., 2000. Coesite inclusions and prograde compositional zonation of garnet in whiteschist of the HP-UHPM Kokchetav massif, Kazakhstan: a record of progressive UHP metamorphism. Lithos 52, 215–233.
Paterson, M.S., 1973. Nonhydrostatic thermodynamics and its geologic applications. Reviews of Geophysics and Space Physics 11, 355–389.
Pattison, D.R.M., De Capitani, C., Gaides, F., 2011. Petrological consequences of variations in metamorphic reaction affinity. Journal of Metamorphic Geology 29, 953–977.
Petrini, K., Podladchikov, Y., 2000. Lithospheric pressure–depth relationship in compressive regions of thickened crust. Journal of Metamorphic Geology 18, 67–77.
Pleuger, J., Podladchikov, Y.Y., 2014. A purely structural restoration of the NFP20-East cross section and potential tectonic overpressure in the Adula nappe (Central Alps). Tectonics 33, 656–685.
Powell, R., 1978. Equilibrium thermodynamics in petrology: An introduction. Harper & Row, Publishers (284 pp).
Powell, R., Holland, T.J.B., Worley, B., 1998. Calculating phase diagrams involving solid solutions via non-linear equations, with examples using THERMOCALC. Journal of Metamorphic Geology 16, 577–588.
Räss, L., 2013. Three-dimensional GPU-accelerated modeling of buoyancy-driven flow under horizontal far-field stress. MSc Thesis, University of Lausanne (77 pp.).
Rosenberg, C.L., Handy, M.R., 2005. Experimental deformation of partially melted granite revisited: implications for the continental crust. Journal of Metamorphic Geology 23, 19–28.
Rutland, R.W.R., 1965. Tectonic overpressures. In: Pitcher, W.S., Flynn, G.W. (Eds.), Controls of metamorphism. Verl. Oliver and Boyd, pp. 119–139.
Rutter, E.H., 1976. The kinetics of rock deformation by pressure solution. Philosophical Transactions of the Royal Society of London A 283, 203–219.
Savenko, S.V., Dijkstra, M., 2004. Sedimentation and multiphase equilibria in suspensions of colloidal hard rods. Physical Review 70, 051401.
Schmalholz, S.M., Podladchikov, Y.Y., 2013. Tectonic overpressure in weak crustal-scale shear zones and implications for the exhumation of high-pressure rocks. Geophysical Research Letters 40, 1984–1988.
Schmalholz, S.M., Podladchikov, Y.Y., 2014. Metamorphism under stress: The problem of relating minerals to depth. Geology 42, 733–734.
Schmalholz, S.M., Medvedev, S., Lechmann, S.M., Podladchikov, Y., 2014a. Relationship between tectonic overpressure, deviatoric stress, driving force, isostasy and gravitational potential energy. Geophysical Journal International 197, 680–696.
Schmalholz, S.M., Duretz, T., Schenker, F.L., Podladchikov, Y.Y., 2014b. Kinematics and dynamics of tectonic nappes: 2-D numerical modelling and implications for high and ultra-high pressure tectonism in the Western Alps. Tectonophysics http://dx.doi.org/10.1016/j.tecto.2014.05.018.
Schmid, D.W., Podladchikov, Y.Y., 2003. Analytical solutions for deformable elliptical inclusions in general shear. Geophysical Journal International 155, 269–288.
Schmid, D.W., Abart, R., Podladchikov, Y.Y., Milke, R., 2009. Matrix rheology effects on reaction rim growth II: coupled diffusion and creep model. Journal of Metamorphic Geology 27, 83–91.
Schreyer, W., 1995. Ultradeep metamorphic rocks: The retrospective viewpoint. Journal of Geophysical Research, Solid Earth 100, 8353–8366.
Smith, D.C., 1984. Coesite in clinopyroxene in the Caledonides and its implications for geodynamics. Nature 310, 641–644.
Tajčmanová, L., Abart, R., Neusser, G., Rhede, D., 2011. Growth of decompression plagioclase rims around metastable kyanite from high-pressure felsic granulites (Bohemian Massif). Journal of Metamorphic Geology 29, 1003–1018.
Tajčmanová, L., Podladchikov, Y., Powell, R., Moulas, E., Vrijmoed, J.C., Connolly, J.A.D., 2014. Grain-scale pressure variations and chemical equilibrium in high-grade metamorphic rocks. Journal of Metamorphic Geology 32, 195–207.
Thomas, J., 1993. A classical representation for a mass based chemical potential. International Journal of Engineering Science 31, 1279–1294.
Turcotte, D., Schubert, G., 2002. Geodynamics. 2nd ed. Cambridge University Press. (848 pp.).
Verhoogen, J., 1951. The chemical potential of stressed solid. Transactions American Geophysical Union 32, 251–258.
Vrijmoed, J., Podladchikov, Y., 2014. Thermodynamic equilibrium at heterogeneous pressure. Geophysical Research Abstracts 16.
Vrijmoed, J.C., Podladchikov, Y.Y., Andersen, T.B., Hartz, E.H., 2009. An alternative model for ultra-high pressure in the Svartberget Fe-Ti garnet-peridotite, Western Gneiss Region, Norway. European Journal of Mineralogy 21, 1119–1133.
Wensink, H.H., Lekkerkerker, H.N.W., 2004. Sedimentation and multi-phase equilibria in mixtures of platelets and ideal polymer. Europhysics Letters 66, 125–131.
Wheeler, J., 1987. The significance of grain–scale stresses in the kinetics of metamorphism. Contributions to Mineralogy and Petrology 97, 397–404.
Wheeler, J., 2014. Dramatic effects of stress on metamorphic reactions. Geology 42, 647–650.
Yang, J.J., Huang, M.X., Wu, Q.Y., Zhang, H.R., 2014. Coesite-bearing eclogite breccia: implications for coseismic ultrahigh-pressure metamorphism and the rate of the process. Contributions to Mineralogy and Petrology 167, 1013.
Young, T.F., Kraus, K.A., Johnson, J.S., 1954. Thermodynamics of equilibrium in the ultracentrifuge. The Journal of Chemical Physics 22, 878–880.
Yund, R., 1986. Interdiffusion of NaSi–CaAl in peristerite. Physics and Chemistry of Minerals 13, 11–16.
Zhang, Y.X., 1998. Mechanical and phase equilibria in inclusion–host systems. Earth and Planetary Science Letters 157, 209–222.